Change in Landslide susceptibility over time in the central Himalayan region: A case study of Siddhababa Area

Indu Gyawali[1], Birasa Malla[2], Khem Nath Poudyal[1], Bhim Kumar Dahal[2],*

[1]Department of Applied Science and Chemical Engineering, Institute of Engineering, Pulchowk Campus, Lalitpur, Nepal

[2]Department of Civil Engineering, Institute of Engineering, Pulchowk Campus, Lalitpur, Nepal

Abstract

The susceptibility analysis is common for the study of landslides in the Himalayas, considering different invariant causative factors. This study's objective is to examine changes in landslide susceptibility within the Siddhababa area by conducting analyses across various time intervals. This area in western Nepal is prone to landslides due to hilly terrain, steep slopes, complex geology, diverse vegetation cover, and extreme weather conditions. This study examines 281 landslides in an area of approximately 257.38 km2, considering 12 causative factors, including three variable factors such as land use, distance to the road, and precipitation, for three different study periods: 2005-2010, 2010-2015, and 2015-2020. For the three study periods, susceptibility analysis, validation, and mapping were performed to prepare susceptibility maps of the study area. The maps were divided into five levels, ranging from very low to very high. The findings show that the high and very high susceptibility levels have increased from 13% to 41% over time, respectively. The changes in the likelihood of landslides are due to both invariant and variable factors such as human activities and climate playing a significant role in altering the susceptibility of the area over time. It is, therefore, essential to comprehend these factors to develop appropriate strategies for mitigating and adapting to the risks posed by landslides and other natural hazards.

Keywords: himalayan landslides, landslide susceptibility analysis, landslide likelihood, landslide susceptibility maps, landslide factors

*Correspondence to: B.K. Dahal
Emails: 076msccd005.indu@pcampus.edu.np (I. Gyawali), 075msgte003.birasa@pcampus.edu.np (B. Malla), khem@ioe. edu.np (K.N. Poudyal) bhimd@pcampus.edu.np (B.K. Dahal)

1. Introduction

Landslides occur when there is an interference in any terrestrial environment by tectonic [1]hazard potential, and topographic evolution. We assess how landslides shape terrain in response to a wave of uplifttraversing the northern California Coast Ranges (United States, climatic [2] and/or human [3] activities. These activities that occurred in the changing climate are studied to pose a direct threat to the frequency occurrence and intensity of landslides, magnifying the risk globally. The Himalayas are susceptible to landslides because of their topography, geology, geospatial location, and climatic conditions [4]to derive a landslide hazard map of the North-West marginal hills of the Achham. Thematic maps representing various factors that are related to landslide activity were generated using field data and GIS techniques. Landslide events of the old landslides were used to assess the Bayesian probability of landslides in each cell unit with respect to the causative factors. Results: The analysis suggests that geomorphological and human-related factors play significant roles in determining the probability value. The hazard map prepared with five hazard classes viz. Very high, High, Moderate, Low and Very Low was used to determine the location of prime causative factors responsible for instability. Spatial distribution of causative factor was correlated with the mechanism and scale of failure. For the mitigation of such shallow-seated failure, bioengineering techniques (i.e. grass plantation, shrubs plantation, tree plantation along with small scale civil engineering structures. The situation is particularly severe in the central Himalayan arc. The region's climate, including precipitation, is heavily influenced by monsoon rainfall, with approximately 80% of the rainfall occurring within around 100 days of the monsoon season [5]. The changing climate further intensifies the dynamic nature of the area, increasing its susceptibility to landslides and rainfall-induced disasters. Additionally, there are anthropogenic factors such as changes in land use and road construction that significantly impact the likelihood of landslides in the region.

Nepal, a country in the Himalayas with a varied topography; 83% of the country is covered by mountains, with the remaining 17% located on the northern edge of the alluvial plains, is prone to multi-hazards [5]. According to Shrestha 2019, Nepal experiences hundreds of destructive landslides and roadside slope collapses every year, which result in enormous losses in lives and property. This is due to the country's vast mountainous terrain, which is mostly highly elevated, rugged, and fragile, along with annual monsoonal heavy precipitations and other dynamic geological processes [6]. In the Nepal Himalaya, rainfall-induced landslides cause severe effects on people, property, infrastructure, and the environment, especially during the monsoon season.

At present, many national highways in Nepal are sporadically facing rock-fall and landslide events, causing fatal accidents at an alarming rate. Siddhartha Highway is one of the highways in Nepal, where tragic rock-fall occurrences have a long history of a significant number of victims [7]. Similarly, the frequent occurrence of landslides around the Siddhababa area during the monsoon causes obstruction of the road, making it difficult to pass by for local walkers, travelers, and tourists. This not only created a noxious environment for travelers, but also invited a great deal of damage to nearby livelihoods and landscapes. Almost every year, accidents and casualties of people walking, working, or driving on this part of the highway are reported. This raises a series of concerns concerning the environment and community under threat from landslide hazards in the area that are poorly understood [8]. Moreover, Nepal has long been experiencing an upsurge in catastrophic landslides, despite very few acknowledgments, particularly in the western part of the country.

According to the IPCC (2007), climate change is characterized as a long-term change in temperature and weather patterns [9]. Climate change includes large-scale changes in weather patterns that come from both global warming and human-caused greenhouse gas emissions. Due to the small number of scientific research undertaken in this region, including Nepal, the IPCC's Fourth Assessment Report identified this region as a "white spot" [9]. From 1971 to 2005, the average temperature in Nepal rose at a steady and continuous pace of 0.05℃ per year, according to the Department of Hydrology and Meteorology (DHM). Between 1975 and 2005, the maximum temperature rose by 0.06℃ each year, while the lowest temperature increased by 0.03℃ per year
[10]. Similarly, Nepal's annual average rainfall is increasing by 13 mm, although the number of wet days is falling by 0.8 days every year. A study of monsoon rainfall from 1971 to 2005 found a linear increasing trend of roughly 2.08 mm/year with significant inter annual variance [11].

Concern over the potential impact of climate change on landslides has risen in recent years. Changes in precipitation patterns, increased intensity and frequency of extreme weather events, and changes in soil moisture content have been studied to analyze the occurrence and magnitude of landslides. [12] used well-established techniques and models to investigate the possible impact of climate change on landslide occurrence and hazard in Central Italy. The study attempted to establish a cause-and-effect relationship between climate

change forecasts and landslide occurrence by building synthetic downscaled rainfall fields, defining rainfall thresholds, and modeling slope stability caused by rainfall events. It is crucial to note that the links between climate change and landslides are complicated and still not understood. While some research has shown a connection between landslides and climate change, others have found no conclusive evidence of one [13. To fully understand the effects of climate change on landslides and to create practical mitigation methods, the subject requires a comprehensive study.

In numerous studies conducted over the past few decades, land use has consistently been considered a significant causative factor in landslide susceptibility. However, despite its recognized importance, the exploration of land use changes in landslide susceptibility analysis has been limited, leaving a significant potential for future research [14]. While, the rapid expansion of urbanization has led to the conversion of substantial areas of forested and cultivable land into urban fringes. This transformation, combined with the challenging terrain and complex topography, has significantly increased the occurrence of landslides caused by human interventions [15]. Moreover, recognizing the importance of land use in landslide assessment requires examining the influence of human activities on slopes, particularly agricultural and forestry practices [14]. These activities are further influenced by climate change, emphasizing the need for effective management strategies to minimize landslide susceptibility [13. However, limiting landslide assessments to past conditions provides a narrow perspective since human activities significantly alter hillside conditions [4], [16]. Therefore, incorporating changing land use scenarios into landslide susceptibility analysis can yield more practical outcomes. This approach assists public administrators in long-term land use management and reduces the risk of landslide disasters.

Landslide susceptibility analysis is commonly conducted in the Himalayas, taking into account various invariant factors, but no previous studies have considered the variable parameters and their effects. This research aims to bridge this gap by conducting a landslide susceptibility analysis that incorporates variable factors and evaluates their impacts. The study also highlights the impact of climate change on landslide susceptibility in the study region.

1. Materials and methods

1.1 Study Area

The study area lies in the Palpa and Rupandehi districts of the Lumbini Zone of western Nepal in Province 5. The total coverage of the study region is 257.38 km2. It extends within latitudes 27°40′12″ N to 27°49′48″ N and longitudes 83°20′24″ E to 83°35′24″ E (Fig. 1). It is bounded by Butwal Nagarpalika and Tinau Gaupalika.
It touches the east-west highway stretch and the Siddhartha Highway. The study area lies in the middle of the mountainous region of western Nepal. The elevation of the study area varies from 55 to 1647 m above mean sea level (masl). The Siddhartha Highway that falls under the study area follows the main watercourse of Tinau Khola, bounded by the Siwalik range in the south. The study area has highly rough terrain with steep slopes and a deeply incised valley of Tinau Khola. This area bounded by the Tinau watershed is tectonically active and geomorphologically very unstable as well because of its location lying in between the main boundary thrust (MBT) and the central boundary thrust (CBT) [7].
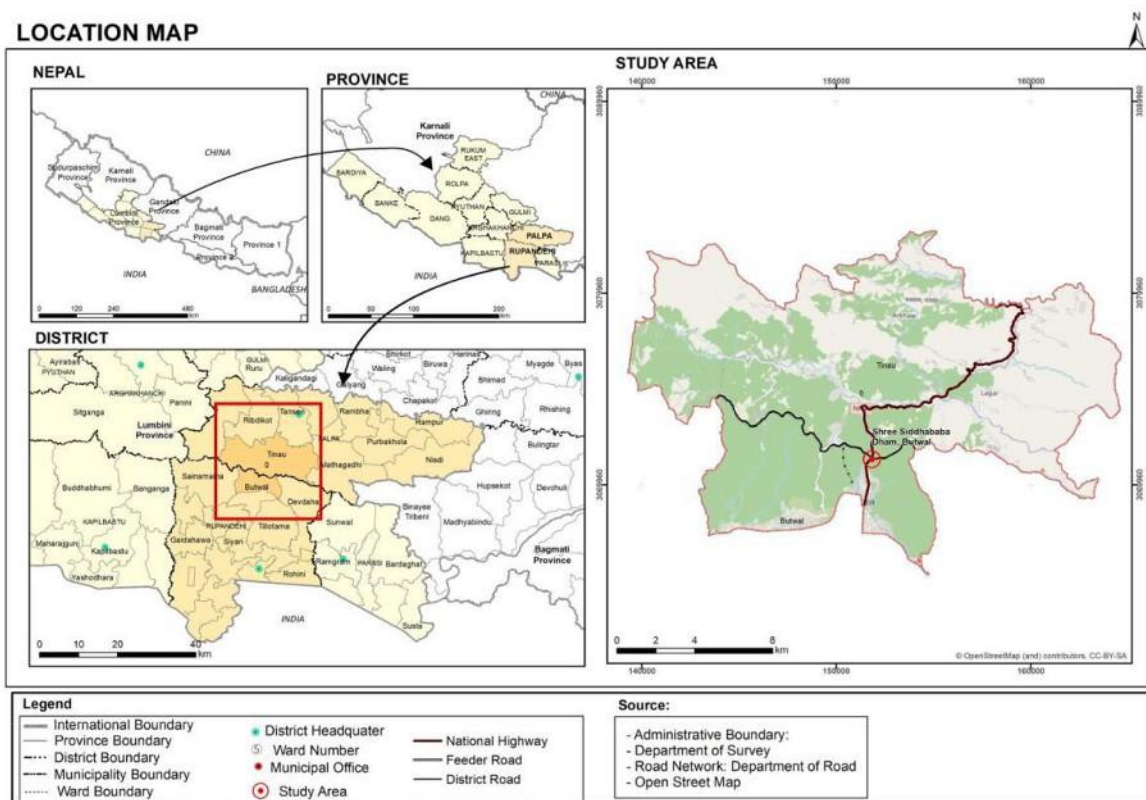
Fig. 1 Location of the study area

The study area falls under two climatic zones: the sub-tropical zone and the warm temperate humid zone. Since our study area is the administration boundary between Palpa and Butwal, the data used in this study are taken from two stations: Butwal and Tansen. Precipitation data were collected from the Department of Hydrology and Meteorology (DHM). Details about the hydrological and meteorological stations are presented in Table 1.

Station No.	Location	Co-ordinate		Elevation (m)	Measuring station type
		Latitude	Longitude		
702	Tansen	27° 51′ 36″	83° 32′ 24″	1187	Climatology Manned
703	Butwal	27° 41′ 24″	83° 27′ 36″	205	Climatology Manned

Data and Sources

For this study, different sets of data, such as DEM, precipitation, land cover, lithology, and relative relief, are required, which are obtained from various organizations. A 12.5 x 12.5 m resolution Digital Elevation Model (DEM) was derived from the USGS (United States Geological Survey, https://earthexplorer.usgs. gov/). A Digital Elevation Model (DEM) is a three-dimensional or digital model of a terrain's surface created using elevation data. The elevations of the Earth's surface, as well as the location of natural and associated features, are determined using DEM data. SRTM and Advanced Spaceborne Thermal Emission and Reflection Radiometer (ASTER) DEMs with a resolution of 12.5 m are widely available in Nepal. The use of ASTER 12.5 m DEM in this study was accompanied by a series of errors while processing in ArcMap, which made the selection of SRTM DEM more reliable.

1.2 **Landslide Susceptibility Analysis**

Fig. 2 presents a framework that was developed specifically for this investigation, which uses indicators to assess various causal factors. These factors were selected based on a literature review, their relevance to the study area, and the availability of data.
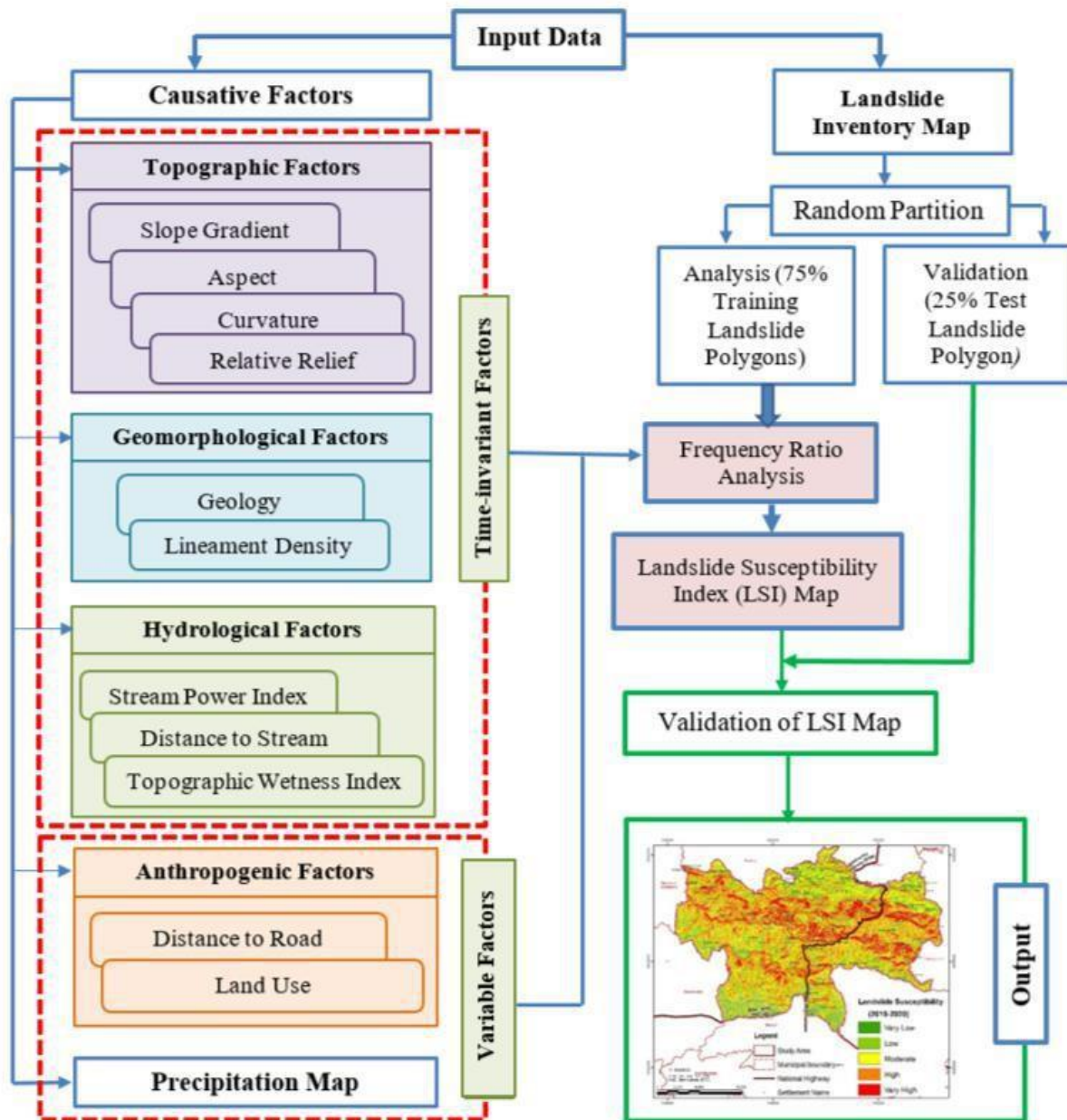
Fig. 2 Flow chart showing data inputs to produce landslide susceptibility maps

The weighting of the selected conditioning factors is part of the landslide susceptibility mapping procedure. Landslide susceptibility analysis weight calculation can be done using a variety of statistical methods. The frequency ratio approach is utilized in this study to identify the link between landslide location and factors in the study area. It is based on the observed relationships between landslide distribution and each landslide-related factor[17]Malaysia using Geographic Information System (GIS. To obtain the Landslide Susceptibility Index (LSI), the ratings of the factors were summed as:

$$LSI = \sum (FR)_i \quad (i = 1,2,3,\dots\dots.n)$$

where, FR_i = Frequency Ratio of factors i.

To determine the probabilistic link between dependent and independent variables, including multi-classified maps, a FR model can be used as a simplified geospatial assessment tool [18]Janghung and Boeun, Korea, using the geographic information system (GIS. The FR approach is easy to use, and the outcomes are simple to comprehend[19], [20]processed, and constructed into a spatial database using GIS and image processing. The factors chosen that influence landslide occurrence were: topographic slope, topographic aspect, topographic curvature and distance from drainage, all from the topographic database; lithology and distance from lineament, taken from the geologic database; land use from Landsat Thermatic Mapper (TM. The FR is defined as the ratio of the region where landslides have occurred to the overall study area, and the ratio of the probability of a landslide occurrence to the chance of nonoccurrence for a particular attribute [19]processed, and constructed into a spatial database using GIS and image processing. The factors chosen that influence landslide occurrence were: topographic slope, topographic aspect, topographic curvature and distance from drainage, all from the topographic database; lithology and distance from lineament, taken from the geologic database; land use from Landsat Thermatic Mapper (TM. To compute the FR, the area ratio of occurrence of landslides to nonoccurrence was determined for each class, followed by an area ratio of the class to the total area.

$$FR = \frac{N_i^p / N}{N_i^{lp} / N^l}$$

Where, N_P = Number of pixels in each factor class i

N = Number of all pixels in the whole study area

N_{lP} = Number of landslide pixels in each factor class i

N_l = Number of all landslide pixels in the whole study area

Using the above equation, frequency ratio for each conditioning factor is calculated. After that, the relative frequency (RF) is calculated to normalize the FR and its value ranges between 0 and 1.

The mathematical expression for RF calculation is:

$$RF = \frac{FR_i}{\sum_i^n FR}$$

Where FRi = Frequency ratio of each class in conditioning factor

FR = Total sum of Frequency ratio of each class in the conditioning factor

Relative frequency has the drawback of weighing all conditioning factors equally [21]. To solve this flaw, the prediction rate (PR) is determined for all factors, taking into account their mutual interaction. For the calculation, the following equation was used.

$$PR = \frac{Max\ RF - Min\ RF}{Min\ (Max\ RF - Min\ RF)}$$

Finally, a landslide susceptibility map (LSM) was created in ArcGIS 10.8 using the raster calculator by combining conditioning factors classed according to their RF values and multiplying each value by its appropriate PR value.

$$LSI = \sum (PR \times RF)$$

After classifying the landslide susceptibility index value into five ranges very low, low, moderate, high, and very high, a landslide susceptibility map was produced. The susceptibility map was validated with a typical area under curve by superimposing these maps with landslide inventory maps.

2. **Result and Discussions**

1.1 **Landslide Inventory Map**

With the processing of image, data inputs and a thorough study, a landslide inventory map for the study area that lies under Palpa and Rupandehi district was prepared as presented in Fig. 3. Visible scars from landslides were first outlined using Google Earth for landslide inventory mapping into GIS. To create a landslide inventory map, news coverage from the Siddhababa area were also taken into account along with satellite imagery. The map indicates the location of historical landslide events, denoted by red dots. A total of

281 landslides were identified, 66 in SP-I, 76 in SP-II, and 139 in SP-III.
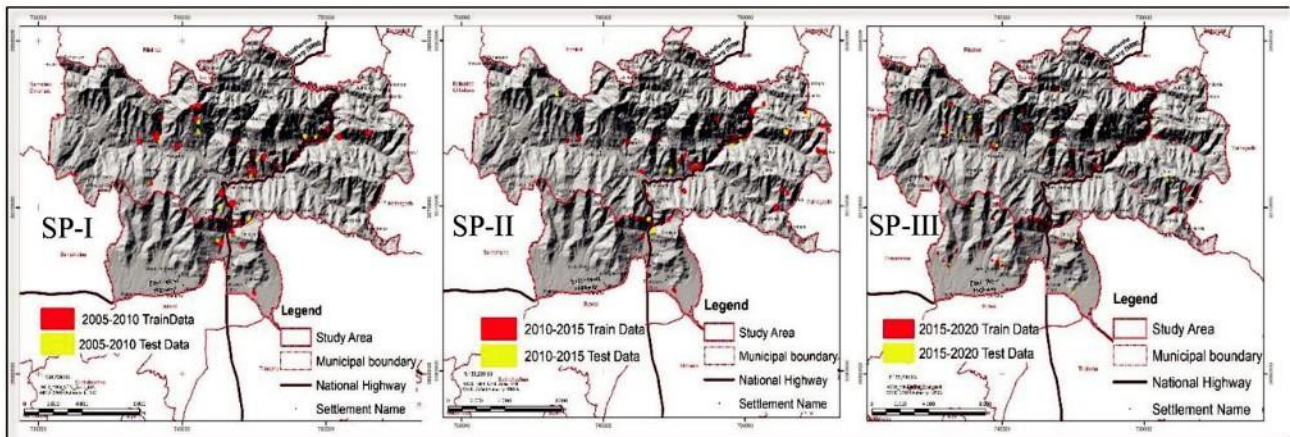
Fig. 3 Landslide Inventory Maps

1.2 **Causative Factors**

The total of 12 factors used in this study for landslide susceptibility mapping. These factors can be categorized into five groups: Topographic, Geomorphological, Hydrological, Anthropogenic and Climatic Factors. The first three groups are considered as factors of time invariance, while the latter two are considered variable factors.

1.2.1 **Topographic Factors**

Topographical factors such as slope, aspect, curvature, and relative relief are prepared using the spatial analyst tool in ArcGIS 10.8w from the DEM of the study area.
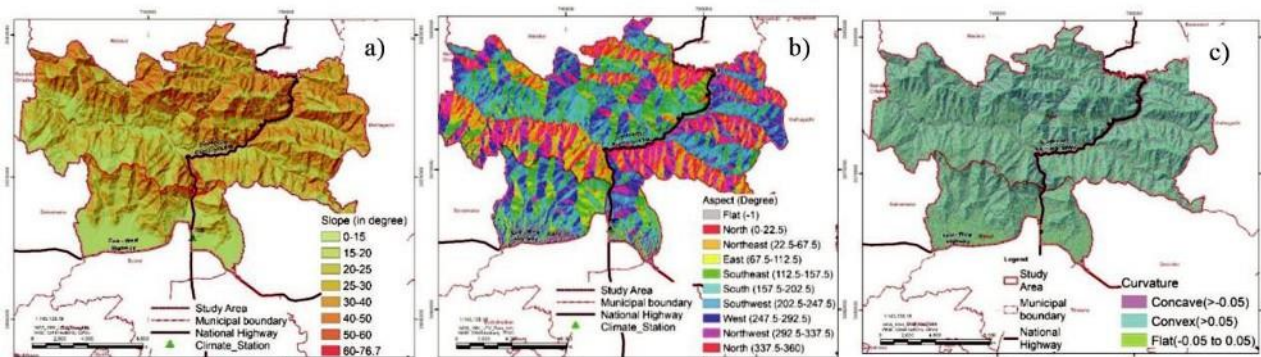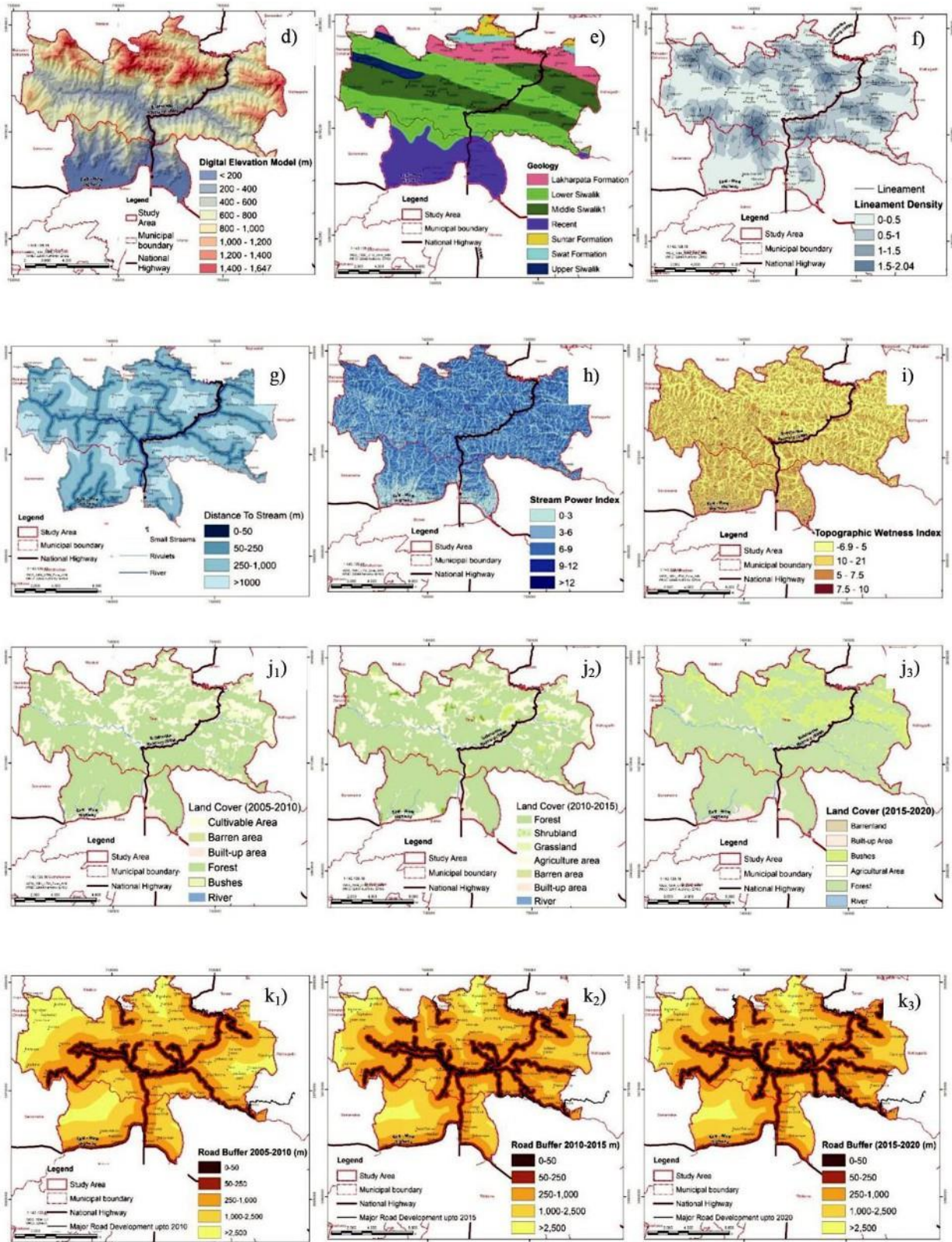
Fig. 4 Factor Maps : (a) Slope , (b) Aspect, (c) Curvature , (d) DEM , (e) Geology, (f) Lineament density, (g) Distance to Stream , (h) SPI, (i) TWI , (j1) LULC: SP-I , (j2) SP-II, (j3) SP-III ; (k1) Road buffer: SP-I, (k2) SP-II, (k3) SP-III,

Slope

The slope values ranges from 0 to 90 degrees and divided into eight categories, namely 0-15˚, 15˚-20˚, 20˚-25˚, 25˚-30˚, 30˚-40˚, 40˚-50˚, 50˚-60˚, and 60˚-76.70˚ (Fig. 4a). The slope FR value revealed that the areas with the highest susceptibility were those with slopes of 50-60 degrees for SP-I and SP-II, while for SP-III, it was 40-50 degrees. The study results imply that the susceptibility to landslides increases up to a certain value as the slope gradient rises due to the changes in slope material and its characteristics.

Aspect

The slope aspect was classified into nine classes, including north, northeast, east, southeast, south, southwest, west, northwest, and North (Fig. 4b). According to the results, the slopes facing the southeast, south and southwest had higher FR values for the studied periods. Various factors, such as exposure to solar radiation, soil properties, drainage, and vegetation cover on slopes, could contribute to this pattern.

Curvature

The curvature map that was prepared was categorized into three groups: Concave (< -0.05) Flat (0.05 -0.05), and Convex (> 0.05) (Fig. 4c). When it comes to curvature, the FR values of Concave (>-0.05) and Convex (>0.05) surfaces are higher than those of Flat surfaces. This is because concave and convex surfaces have steep slopes that can cause water concentration and soil movement, making them more susceptible to landslides [22] Conversely, flat surfaces have lower slopes and are less likely to experience landslides. Additionally, concave and convex surfaces can create small topographic depressions that can accumulate water and increase soil saturation, thereby raising the risk of landslides [22].

Relative relief

The relative relief was divided into eight classes: 55-200 m, 200 - 400 m, 400 - 600 m, 600-800 m, 800-1000 m, 1000-1200 m, 1200-1400 m, 1400-1647 m (Fig. 4d). In case of relative relief, the 1400-1647 m class has a higher FR value for the studied period. This may be due to the presence of steep slopes and an increased risk of landslides in such areas. Furthermore, areas with high relief are more likely to undergo changes in soil type, lithology, and vegetation cover, which can make them more susceptible to landslides. Furthermore, high-relief areas tend to have higher levels of rainfall and water infiltration, which can lead to soil saturation and landslides [22].

3.2.2 Geomorphological Factors

Geology

The ICIMOD digitized map (https://rds.icimod.org/) using the Soil Terrain Database (SOTER, 2009) and the geology map of Nepal from the Department of Mines and Geology (DMG) of Nepal (https://www.dmgnepal.gov.np/map), which was processed in ArcGIS 10.8. The map identified several geological formations, such as the Lakharpata Formation, Lower Siwalik, Recent Deposits, Swat Formation, Suntar Formation, Upper Siwalik, and Middle Siwalik, and classified them accordingly (Fig. 4e). Based on the FR value, the Middle Siwalik Formation showed the highest value among the geological formations for all study periods due to the geological properties of this region. The Middle Siwalik Range is made up of sandstones, siltstones, and mudstones, sedimentary rocks that are easily weathered, making them susceptible to landslides due to weak interlayer bonds and poor strength. Furthermore, this area experiences high rainfall, which can further increase the vulnerability of geological formations and trigger landslides.

Lineament Density

The spatial analyst tool in ArcGIS 10.8 was used to generate the lineament density map (Fig. 4f) from the lineament map. Lineament density was categorized into four ranges: < 0.5, 0.5 - 1.0, 1.0 - 1.5, and 1.5 - 2.04. Lineament density classes have varying effects on slope stability and landslide susceptibility. The 0-0.5 density class showed higher stability during SP-I and SP-II, indicating lower fracturing and faulting, which may lead to less groundwater storage and less pore pressure, stabilizing the slope. However, the 1-1.5 density class had higher susceptibility during SP-III, possibly due to increased pore pressure caused by changing climatic conditions, which can increase pore pressure in slopes with a higher degree of fracturing and faulting, making them more prone to landslides.

3.2.3. Hydrological Factors

Distance to Stream

The DEM of the study area was used to generate a stream network map in ArcGIS 10.8, using the flow accumulation map. Then, the spatial analyst tool was employed to create a distance to stream map (Fig. 4g), which was subsequently divided into four classes: 0-50 m, 50-250 m, 250-1000 m, and >1000 m. During the study periods, the range of 50-250 m exhibited higher FR values compared to the other classes. This finding could be attributed to several factors. Firstly, locations within this range may be more susceptible to high water flow or flooding during severe rainfall events, which could increase the likelihood of landslides. Second, the range may indicate areas with steeper topography or incised channels, which could increase the susceptibility to landslides

Stream Power Index

The stream power index (SPI) is a measure of the erosive power of flowing water. This index is computed based on the slope and the contributing area, and it provides an approximation of where gullies are more likely to develop. SPI is calculated using the following equation:

$$SPI_i = ln(DA_i * tan(G_i))$$

Where, SPI is the stream power index at grid cell, is the upstream drainage area (flow accumulation at grid cell multiplied by grid cell area), is the slope at grid cell in radians.

The stream power index map (Fig. 4h) for the study area was generated using the ArcGIS raster tool and divided into five classes: 3, 6, 9, 12, and greater than 12. Based on the FR values, the class range of 6-9 showed a higher susceptibility to landslides compared to areas with lower or higher values. The reason for this may be attributed to the ideal combination of slope materials, drainage area, slope gradient, and channel gradient in regions with the class.

Topographic Wetness Index (TWI)

The topographic wetness index (TWI) is commonly used to measure the impact of topography on hydrological processes and describes the distribution of soil moisture. TWI is calculated using the formula:

$$TWI = ln\, a/tan\, \beta$$

Where, a represents the accumulated upslope area draining through a point and tan is the slope angle at that point. In this study, the TWI map (Fig. 4i) of the study area was generated using the raster tool in ArcGIS and was classified into four categories: -6.9-5, 5-7.5, 7.5-10, and 10-21. The FR distribution showed that TWI class ranges of -6.9-5 and 5-7.5 had higher values for all study periods. This indicates that these areas have moderate

to high potential for water accumulation, which can lead to increased soil saturation and decreased soil stability, thus increasing the likelihood of landslides in these regions.

3.2.4 Anthropogenic Factors

Land Use

The ICIMOD Regional Database System (https://rds.icimod.org/) was used to obtain a land use and land cover map of Nepal. The acquired map was then processed in ArcGIS 10.8. The land use land cover was divided into six classes: Water bodies, Bushes, Forest, Cultivable land, Built-up and Barren land (Fig. 4j1, j2, j3). For Land use, bushes and barren land have higher FR values in SP-I and SP-III, while for SP-II, bushes and agricultural land contributes to higher FR values. This could be attributed to changes in practices for land use and management over time.

Distance to Road

The distance to the road map was prepared from the road network map obtained from the Humanitarian Data Exchange, which combined data from the Department of Survey, Nepal, with information from the SRN Strategic Road Network 2016. The map is further classified into five classes: 0-50m, 50-250m, 250-1000m, 1000-2500m and over 2500m (Fig. 4k1, k2, k3). FR analysis infers that for SP-I and SP-II, the class range of 50-250m has a higher value, while for SP-III, the range of 250-1000m has a higher value. This could be because there was more human activity and development within 50-250m of the roads in the past, which increased the chance of landslides in that area. However, in more recent times, human activity and development may have spread to locations further from highways, resulting in higher FR values in the range of 250 to 1000 m.

3.2.5 Climatic Factors

Precipitation

A change in the pattern of rainfall over time refers how the climate change has imposed on the climatic variables. To determine the annual precipitation in a particular area between 2005 and 2019, data was collected from two meteorological stations, Station 702 and Station 703, located in Palpa and Rupandehi, respectively. The study period was divided into three periods, labeled Study Period I (SP-I), Study Period II (SP-II), and Study Period III (SP-III) from 2005-2010, 2010-2015, and 2015-2020, respectively. The study focused on the maximum amount of rainfall since this is a significant factor in causing landslides. Daily and monthly maximum precipitation values were analyzed, as shown in Fig. 5 and Fig. 6. The graphs demonstrate that there is no consistent pattern in the daily rainfall data over time, but there is an overall increase in the monthly precipitation values from the base year to the observed year period. This suggests that rainfall patterns are changing with time due to the impact of climate change on climatic variables.
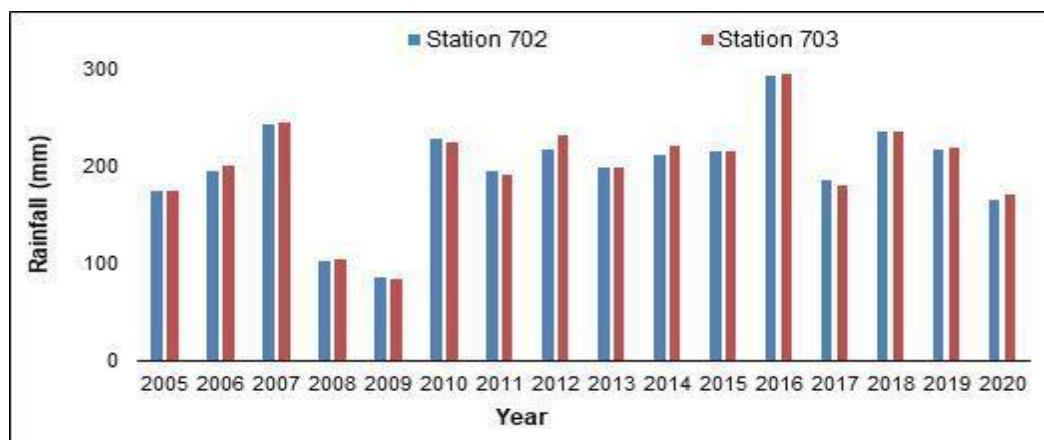
Fig. 5 Daily Maximum Rainfall
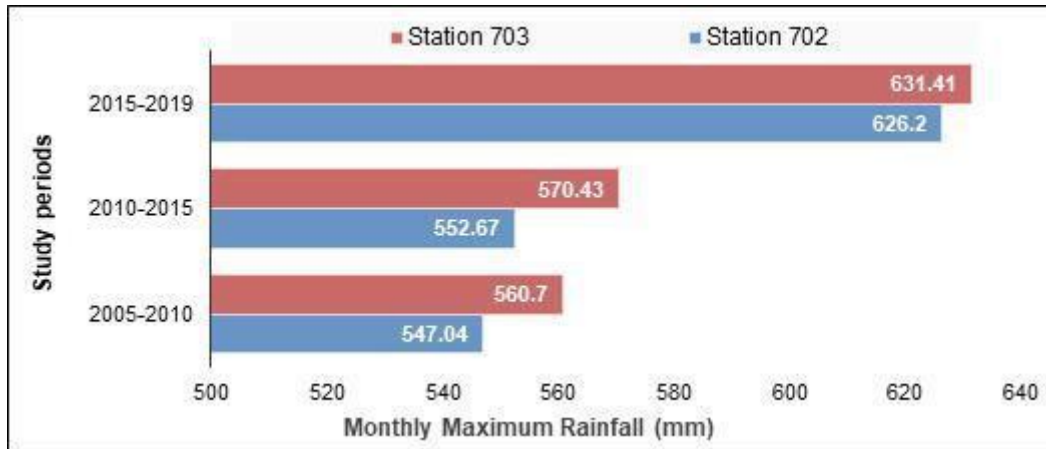
Fig. 6 Monthly Maximum Rainfall

Stations No. 702 and 703, located close to the research area, were used to create a precipitation map and divided into five classes (Fig. 7l1, l2, l3). The FR value was found to be higher for the class range of 243.9-244.1 mm during SP-I, less than 229.5 mm in SP-II, and less than 293.0 mm in SP-III. The variation in FR values for different precipitation ranges in different time periods may be due to the unique topographical and geological characteristics of the research area and its local rainfall patterns. The daily maximum rainfall varied across the study periods, and the increasing monthly maximum value over time suggested that cumulative rainfall played a crucial role in causing landslides in SP-III.
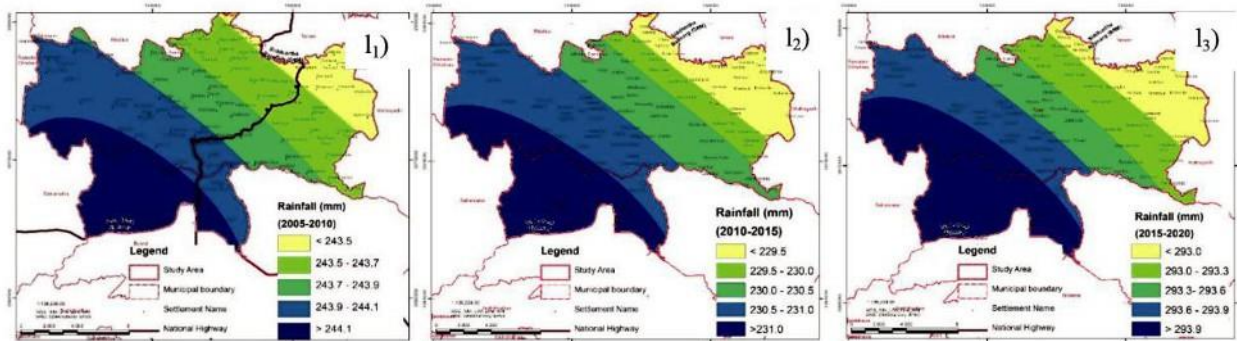
Fig. 7 Rainfall Maps: SP-I, l2) SP-II, l3) SP-III

The variable causative factors are presented in the Table 2 below. The data reveals that over time, there was a significant reduction in the amount of cultivated land, and a corresponding increase in the built-up areas, forests, and bushes. Additionally, the distance from the road had a significant impact, as areas within 1km of a road increased from 47% to 62%. These changes in land use, along with the construction of new roads and the higher levels of precipitation, are all factors that contributed to the occurrence of landslides.

Table 2 Variable factors for different study periods

Causative Factors	Class	Area (%)		
		SP-I	SP-II	SP-III
Land use	Bushes	1.82	3.03	18.82
	Forest	71.37	72.52	75.20
	Cultivable Area	24.06	21.35	0.49
	Built up	1.04	1.09	4.00
	Water Bodies	1.38	1.38	1.38
	Barren land	0.33	0.62	0.10
Distance to Road (m)	0-50	4.03	5.64	6.05
	50-250	11.99	16.01	16.80
	250-1000	31.74	38.60	39.24
	1000-2500	36.62	32.14	30.30
	>2500	15.63	7.61	7.61
Precipitation	Class-I	9.61	7.63	4.93
	Class-II	20.46	15.72	18.58
	Class-III	16.49	14.54	20.11
	Class-IV	30.71	28.96	29.40
	Class-V	22.73	33.15	26.99

1.3 Landslide Susceptibility Analysis

In this research, the frequency ratio model was used to assess the probability of landslides by analyzing twelve specific factors and comparing them with previous landslide occurrences. The relationship between these factors and landslides was determined by their frequency ratio values; a higher value indicating a higher susceptibility to landslides. The PR and FR values were calculated for each class using a 75% training dataset after conditioning the factors. A high PR value for a factor indicates a strong correlation with the occurrence of landslides in the area. The results showed that the PR values for each factor differed during the three study periods, with land use becoming increasingly important over time. Other factors, such as slope, distance to the stream, geology, and precipitation, also showed changes in their PR values, with some increasing and others decreasing. Fig. 8 depicts the predictive rate of all twelve causative factors, indicating dynamic nature and their importance over time.

	Slope	Aspect	Landuse	D to R	D toS	Relative Relief	Curvature	Geology	Lineament Density	SPI	TWI	Precipitation
SP-I	4.65	3.50	5.20	4.84	6.04	4.06	1.00	5.85	5.28	2.99	4.03	5.57
SP-II	4.02	1.49	3.18	1.00	1.26	3.20	1.26	3.47	2.67	1.63	1.77	3.87
SP-III	2.83	3.25	10.12	1.42	2.44	2.76	1.00	3.92	2.74	4.76	3.23	6.11
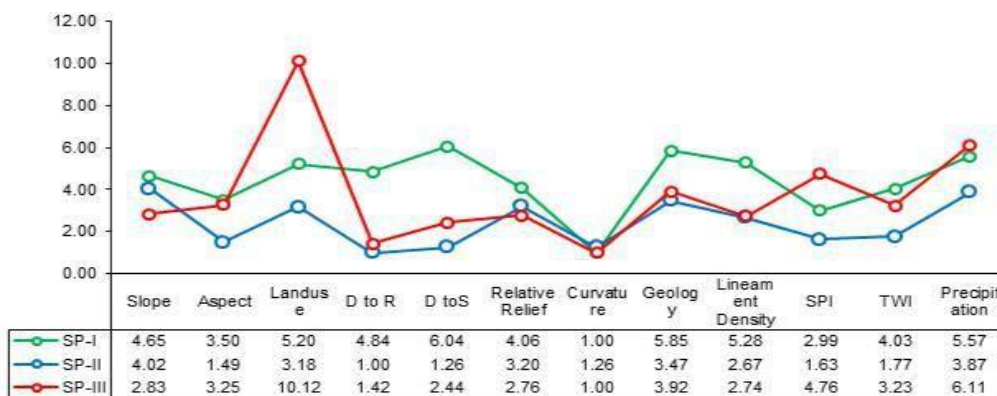
Fig. 8 Predictive rate of causative factors

The susceptibility weight for each factor was calculated by multiplying their FR values by PR. This process was repeated for all factors, and the resulting weight maps were plotted as raster maps. These maps were then added together to generate the Landslide Susceptibility Index (LSI) map, which is presented in Fig. 9.
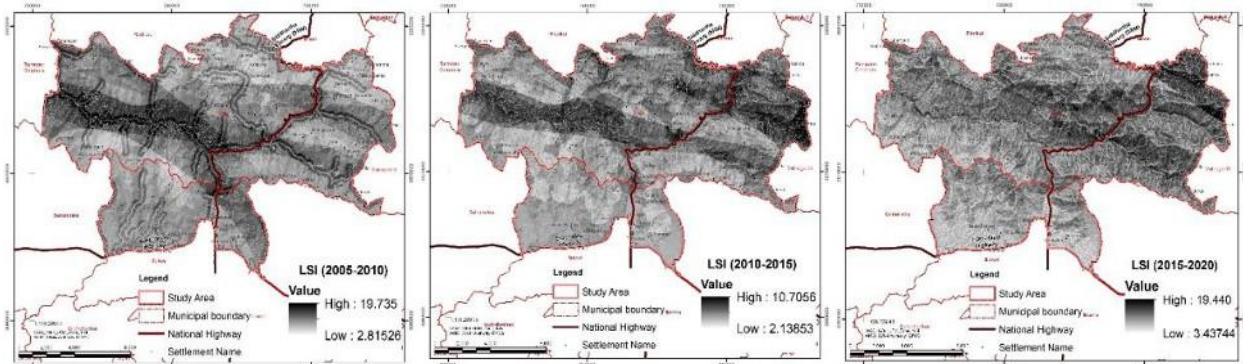
Fig. 9 Landslide Susceptibility Index Maps

3.3.1 Validation

Measures of the goodness of fit and predictive power of the susceptibility model are tested using independent populations of landslides [23]. The susceptibility model is compared with the randomly selected training and testing set, i.e., 75% and 25% of total landslides. The presence of these landslides sets a higher LSI value, which shows higher success and prediction rates [24]it is part of the northwestern highlands of Ethiopia. This area is part of the Guna Mountain which is characterized by weathered volcanic rocks, rugged morphology with deeply incised gorges, heavy rainfall and active surface processes. Many landslides have occurred on August 2018 after a period of heavy rainfall and they caused many damages to the local people. In this study, Frequency Ratio (FR. The area under the curve (AUC) of the graphs prepared using the training and testing data sets and the reclassified landslide susceptibility map produce success and prediction rates, respectively, as illustrated in Fig. 10 for all study periods.

The results showed that the model's performance was consistent over time, with success rates ranging from 82.73% to 84.56% and prediction rates ranging from 78.98% to 79.77%. These figures indicate that the model was able to accurately classify a significant portion of the validation data set and had a high degree of success in predicting where landslides would occur. Overall, the goodness of fit and predictive power measures suggest that the prepared susceptibility model was effective in assessing landslide susceptibility.
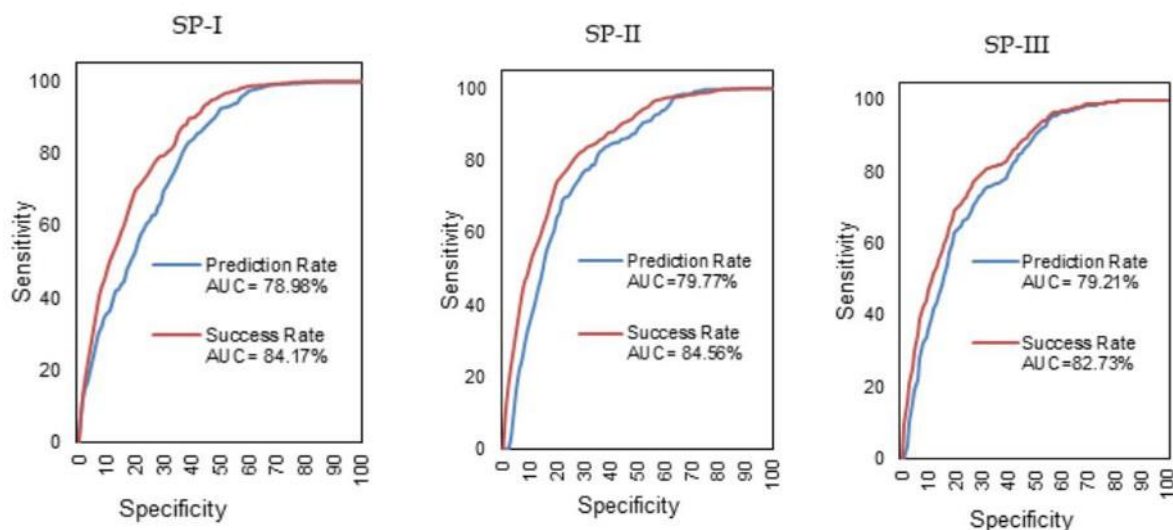
Fig. 10 Success rate and prediction rate for different study periods

3.3.2. Classified Landslide Susceptibility Maps

The landslide susceptibility map is categorized into five classes: very low, low, moderate, high and very high, using the Jenks natural break classification method in GIS. Fig. 11 shows the landslide susceptibility maps for three study periods. From the Table 3, it can be observed that the percentage coverage of the very low susceptibility classification has decreased from 2% in SP-I to 1% in SP-III. In contrast, the percentage coverage of the high and very high susceptibility classifications has increased, with the high susceptibility classification increasing from 12% to 32% and the very high susceptibility classification increasing from 2% to 9% over the same time period. The region covered by very low susceptibility landslides is decreasing as more and more land becomes vulnerable to moderate to high susceptibility landslides. This demonstrates how the region becomes increasingly vulnerable to landslides as the year progresses.

The variable factors and their characteristics, like shifts in land use patterns, climatic circumstances, distance to roads (see, Table 2) and other runoff related factors are the reason for these changes. Landslides, for example, may occur more frequently if urbanization or deforestation increases in a specific area. Similarly, heavy rainfall or changes in topography can also affect the susceptibility of an area to landslides.
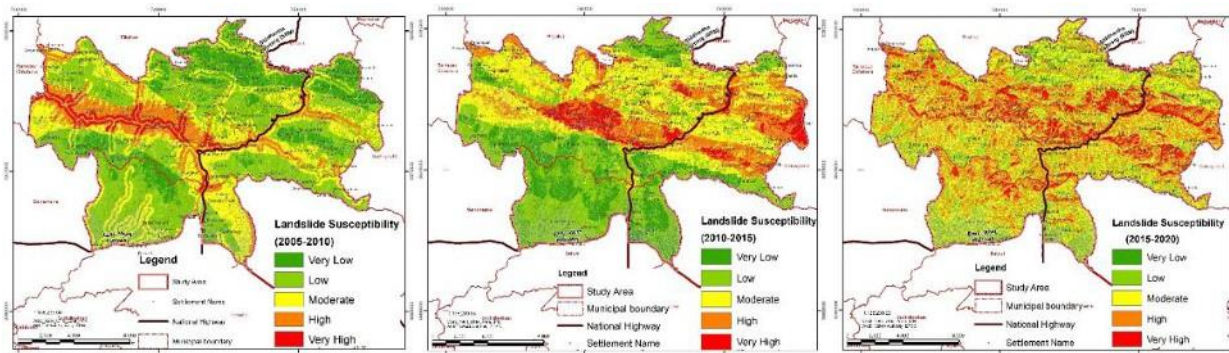
Fig. 11 Classified susceptibility maps for different study periods

Table 3 Landslide affected area for different susceptibility levels from 2005-2020

S.N.	Susceptibility Classification	2005-2010		2010-2015		2015-2020	
		Area (sq. km)	Percentage Coverage	Area (sq. km)	Percentage Coverage	Area (sq. km)	Percentage Coverage
1	Very Low	4.187	2%	34.156	16%	3.127	1%
2	Low	94.959	44%	66.161	30%	38.909	18%
3	Moderate	88.599	41%	61.756	28%	86.549	40%
4	High	25.295	12%	40.910	19%	71.173	32%
5	Very High	3.991	2%	14.050	6%	19.251	9%

3. Conclusions

The Siddhababa Area, which lies in the western region of Nepal within the administrative borders of Palpa and Rupandehi, is susceptible to landslides due to a combination of factors such as steep slopes, complex geology, diverse vegetation cover, and extreme weather conditions like heavy rainfall. This study investigates 281 landslides in an area of approximately 257.38 km2 over three different periods (2005-2010, 2010-2015, and

2015-2019), taking into account 12 factors, including three variable factors such as land use, distance to the road, and precipitation. Some of the major conclusions drawn from this study are as follows:

- The precipitation data of stations 702 (Palpa) and 703 (Rupandehi) reveal that the change in maximum monthly rainfall increases by approximately 100 mm for both stations over time. This trend is expected to increase with a changing climate and poses a high risk of occurrence in the study region.

- The variable factors considered in this study revealed that the expansion of built-up land, the decrease in the distance to newly constructed roads, and the increase in precipitation are the main reasons for the increase in the area classified as having a high or very high susceptibility.

- Susceptibility is classified into five levels: very low, low, moderate, high, and very high. For the study period 2005-2010, 45.7% of the area had very low susceptibility, while moderate susceptibility accounted for 40.8%, and high to very high susceptibility accounted for 13.5%.

- Similarly, for the next study period (2010-2015), the percentage of the area with low and very low susceptibility coverage remained the same at 46.2%, whereas moderate susceptibility coverage dropped to 28.5% and high to very high susceptibility coverage increased to 25.3%.

- In the period from 2015 to 2020, the area with low and very low susceptibility coverage decreased to 19.2%, while moderate coverage increased to 39.5%. The very high susceptibility coverage rose to 41.3%.

- The threefold increase in high and very high susceptibility coverage over the years highlights the need for better land-use management approaches. Such practices should attempt to minimize disturbance to natural landscapes, avoid soil erosion, and maintain soil stability.

Conflict of interest

The authors declare that they have no conflict of interest.

References

[1]   G. L. Bennett, S. R. Miller, J. J. Roering, and D. A. Schmidt, "Landslides, threshold slopes, and the survival of relict terrain in the wake of the Mendocino Triple Junction," *Geology*, vol. 44, no. 5, pp. 363-366, May 2016, doi: 10.1130/G37530.1.

[2]   S. M. Moreiras, "Climatic effect of ENSO associated with landslide occurrence in the Central Andes, Mendoza Province, Argentina," in *Landslides*, Apr. 2005, pp. 53-59. doi: 10.1007/s10346-005-0046-4.

[3] D. N. Petley *et al.*, "Trends in landslide occurrence in Nepal," *Nat. Hazards*, vol. 43, no. 1, pp. 23-44,

Aug. 2007, doi: 10.1007/s11069-006-9100-3.

[4]   B. K. Dahal and R. K. Dahal, "Landslide hazard map: tool for optimization of low-cost mitigation," *Geoenvironmental Disasters*, vol. 4, no. 1, p. 8, Dec. 2017, doi: 10.1186/s40677-017-0071-3.

[5]   R. K. Dahal, S. Hasegawa, T. Masuda, and M. Yamanaka, "Roadside Slope Failures in Nepal during Torrential Rainfall and their Mitigation Road construction practice in Nepal," *Proc. Interpaevent Int. Symp, Niijigata 2006, Disaster Mitig. debris flow, slope Fail. landslides*, no. July 2014, pp. 503-514, 2006.

[6]   B. R. Shrestha, "An Assessment of Disaster Loss and Damage in Nepal," *Geogr. Base*, vol. 6, pp. 42-51, Oct. 2019, doi: 10.3126/tgb.v6i0.26166.

[7]   K. R. Gnyawali *et al.*, "Rockfall Characterization and Structural Protection in the Siddhababa Section of Siddhartha Highway H10, Nepal," *J. Inst. Eng.*, vol. 11, no. 1, pp. 1-11, Mar. 2016, doi: 10.3126/jie. v11i1.14689.

[8]   B. G. McAdoo *et al.*, "Roads and landslides in Nepal: How development affects environmental risk," *Nat. Hazards Earth Syst. Sci.*, vol. 18, no. 12, pp. 3203-3210, 2018, doi: 10.5194/nhess-18-3203-2018. [9]

D. Reay, C. Sabine, P. Smith, and G. Hymus, "Climate change 2007: Spring-time for sinks," *Nature*, vol. 446, no. 7137. pp. 727-728, 2007. doi: 10.1038/446727a.

[10]   R. P. Upadhayaya and M. P. Baral, "Trends of Climate Change in Some Selected Districts of Western Nepal," *Janapriya J. Interdiscip. Stud.*, vol. 9, no. 1, pp. 148-158, Dec. 2020, doi: 10.3126/jjis.v9i1.35284.

[11] S. K. Baidya, M. L. Shrestha, and M. M. Sheikh, "Trends in daily climatic extremes of temperature and precipitation in Nepal," *Hydrol. Meteorol.*, vol. 5, no. 1, pp. 38-51, 2008.

[12]   M. Alvioli *et al.*, "Implications of climate change on landslide hazard in Central Italy," *Sci. Total Environ.*, vol. 630, pp. 1528-1543, Jul. 2018, doi: 10.1016/j.scitotenv.2018.02.315.

[13]   S. L. Gariano and F. Guzzetti, "Landslides in a changing climate," *Earth-Science Rev.*, vol. 162, pp. 227-252, 2016, doi: 10.1016/j.earscirev.2016.08.011.

[14]   R. Pacheco Quevedo, A. Velastegui-Montoya, N. Montalván-Burbano, F. Morante-Carballo, O. Korup, and C. Daleles Rennó, "Land use and land cover as a conditioning factor in landslide susceptibility: a literature review," *Landslides*, vol. 20, no. 5. pp. 967-982, May 2023. doi: 10.1007/s10346-022-02020-4.

[15]   B. R. Adhikari, S. Gautam, and B. Paudel, "Landslide, Land Cover, and Land use Changes and Its Impacts in Nepal," 2022, pp. 149-164. doi: 10.1007/978-981-16-7314-6_6.

[16]   F. Guzzetti, P. Reichenbach, F. Ardizzone, M. Cardinali, and M. Galli, "Estimating the quality

of landslide susceptibility models," *Geomorphology*, vol. 81, no. 1-2, pp. 166-184, Nov. 2006, doi: 10.1016/j.geomorph.2006.04.007.

[17]   S. Lee and B. Pradhan, "Probabilistic landslide hazards and risk mapping on Penang Island, Malaysia," *J. Earth Syst. Sci.*, vol. 115, no. 6, pp. 661-672, Dec. 2006, doi: 10.1007/s12040-006-0004-0.

[18]   H. J. Oh and S. Lee, "Cross-application used to validate landslide susceptibility maps using a probabilistic model from Korea," *Environ. Earth Sci.*, vol. 64, no. 2, pp. 395-409, Sep. 2011, doi: 10.1007/s12665-010-0864-0.

[19]   S. Lee and J. A. Talib, "Probabilistic landslide susceptibility and factor effect analysis," *Environ. Geol.*, vol. 47, no. 7, pp. 982-990, May 2005, doi: 10.1007/s00254-005-1228-z.

[20]   I. Yilmaz, "GIS based susceptibility mapping of karst depression in gypsum: A case study from Sivas basin (Turkey)," *Eng. Geol.*, vol. 90, no. 1-2, pp. 89-103, Mar. 2007, doi: 10.1016/j.enggeo.2006.12.004.

[21] T. D. Acharya and D. H. Lee, "Landslide Susceptibility Mapping using Relative Frequency and Predictor Rate along Araniko Highway," *KSCE J. Civ. Eng.*, vol. 23, no. 2, pp. 763-776, Feb. 2019, doi: 10.1007/s12205-018-0156-x.

[22]   R. K. Dahal, "Landslide hazard mapping in GIS," *J. Nepal Geol. Soc.*, vol. 53, pp. 63-91, 2017, doi: 10.3126/jngs.v53i0.23808.

[23]   B. Pradhan and M. F. Buchroithner, "Comparison and validation of landslide susceptibility maps using an artificial neural network model for three test areas in Malaysia," *Environ. Eng. Geosci.*, vol. 16, no. 2, pp. 107-126, May 2010, doi: 10.2113/gseegeosci.16.2.107.

[24]   T. Mersha and M. Meten, "GIS-based landslide susceptibility mapping and assessment using bivariate statistical methods in Simada area, northwestern Ethiopia," *Geoenvironmental Disasters*, vol. 7, no. 1, p. 20, Dec. 2020, doi: 10.1186/s40677-020-00155-x.